JOURNAL OF CATALYSIS **167,** 256–265 (1997)
ARTICLE NO. CA971581

Kinetic Analysis of the Decomposition of Nitrous Oxide over ZSM-5 Catalysts

Freek Kapteijn,[1] Gregorio Marbán,* José Rodriguez-Mirasol,† and Jacob A. Moulijn

*Industrial Catalysis, Department of Chemical Engineering, Delft University of Technology, Julianalaan 136, 2628 BL Delft, The Netherlands; *Instituto Nacional del Carbon, Oviedo, Spain; and †Department of Chemical Engineering, University of Malaga, Spain*

Received September 20, 1996; revised December 16, 1996; accepted December 16, 1996

A detailed comparative kinetic analysis has been made of the N_2O decomposition over Co-, Fe-, and Cu-ZSM-5. The effect of partial pressure of N_2O, O_2, CO, and NO, the space time, and temperature have been investigated. The decomposition is first order in N_2O over Fe- and Co-ZSM-5 and has a slightly lower order over the Cu sample. Inhibition of oxygen observed for Cu-ZSM-5 is absent for Co and for Fe at the lower temperatures. N_2O destruction is enhanced by CO for all catalysts and by NO for Fe-ZSM-5 only. In the presence of NO, NO_2 is produced over Fe- and Co-ZSM-5. Over Cu-ZSM-5 the enhancement by CO passes through a maximum as a function of CO pressure due to the strong adsorption at reduced sites. A detailed kinetic model that accounts quantitatively for the observed dependencies and which deviates from the classical model for oxidic systems is advanced. Estimates of the maximum turnover rates for the various model steps range from 10^{-4} to 1 s^{-1}.

1. INTRODUCTION

Nitrous oxide has received increasing attention the past decade, due to the growing awareness of its impact on the environment, as it has been identified as an ozone depletion agent and as a Greenhouse gas (1). Identified major sources include adipic acid production, nitric acid, and fertilizer plants, fossil fuel and biomass combustion, and de-NO*x* treatment techniques, like three-way catalysis and selective catalytic reduction (2, 3).

For the abatement of N_2O emissions one can note much interest in the development of catalysts that decompose nitrous oxide into its elements at rates and conditions that are compatible with the production sources (3, 4):

$$2\,N_2O \rightarrow 2\,N_2 + O_2 \quad (\Delta_r H^\circ(298) = -163\ \text{kJ/mol}). \quad [1]$$

Catalysts include oxides, mixed oxides (perovskites), and zeolites (3). The latter, transition metal ion-exchanged zeolites, have been shown to exhibit high activities for the decomposition reaction (5–11). Most published studies deal with Fe-zeolites (5, 7, 8, 10–13), but also Co and Cu systems exhibit high activities (6, 10, 11). ZSM-5 catalysts are quite active (3) and especially Co-ZSM-5 is most attractive in view of its thermostability (14), while Fe- and Cu-ZSM-5 are shown to be deactivated under hydrothermal conditions (15). Detailed kinetic studies, needed for practical application, have hardly been reported (3, 16), and even less is known of the the influence of other components that may be present, like O_2, CO (16), H_2O, NO, and SO_2 (11). For Fe-zeolites mainly a first order in N_2O and a zero order in O_2 is reported (7, 8, 12), although also a positive influence of O_2 has been found (13). Mechanistic studies mainly concern Fe systems (7, 8, 10, 12).

Classically the reaction over oxidic catalysts is described by adsorption followed by an oxidation of active sites, and a subsequent removal of the deposited oxygen by recombination (Eqs. [2]–[4]). The adsorption (Eq. [2]), and desorption (Eq. [4]), are generally assumed to be in quasi-equilibrium under decomposition conditions:

$$N_2O + * \overset{K_{N_2O}}{\longleftrightarrow} N_2O^* \quad [2]$$

$$N_2O^* \overset{k}{\rightarrow} N_2 + O^* \quad [3]$$

$$2\,O^* \underset{K_{O_2}}{\longleftrightarrow} O_2 + 2^*. \quad [4]$$

For steady-state conditions and assuming a constant number of active sites (17) this yields the rate expression [5], where N_T represents the active site concentration (mol/g_{cat}) and r_{N_2O} the conversion rate of N_2O (mol/s g_{cat}). Depending on the values of the parameters in this expression it can be reduced to simpler forms (3). For weak N_2O adsorption and fast surface oxidation [2] and [3] are often combined to one step:

$$r_{N_2O} = \frac{k N_T K_{N_2O} p_{N_2O}}{1 + K_{N_2O} p_{N_2O} + \sqrt{K_{O_2} p_{O_2}}}. \quad [5]$$

Hall *et al.* (7, 8) found for Fe-Y and Fe-Mor an absence of oxygen inhibition and a pure first order behavior for

[1] To whom correspondence should be addressed. Fax: +31 15 278 4452. E-mail: f.kapteijn@stm.tudelft.nl.

0021-9517/97 $25.00

nitrous oxide, similar to that of Fe-ZSM-5 (12). This can be accounted for only if N_2O adsorption is rate limiting, but then the catalytic sites must be in a reduced state, while it could be observed that the catalyst contained a lot of oxygen. Therefore they proposed [7] as the irreversible oxygen removal reaction, in combination with the oxidation step of Eq. [6], resulting in Eq. [8] for the total N_2O conversion rate:

$$N_2O + {}^* \xrightarrow{k_1} N_2 + O^* \quad [6]$$

$$N_2O + O^* \xrightarrow{k_2} N_2 + O_2 + {}^* \quad [7]$$

$$r_{N_2O} = \frac{2k_1k_2N_T}{k_1 + k_2} \cdot p_{N_2O} = \frac{2k_1N_T}{k_1/k_2 + 1} \cdot p_{N_2O}. \quad [8]$$

The ratio k_1/k_2 in Eq. [8] equals $[O^*]/[^*]$ and so determines the state of the active sites. For $k_1/k_2 \gg 1$ the difficult step is Eq. [7] and the sites are oxidized, while for $k_1/k_2 \ll 1$ the reverse holds.

The deposited oxygen, often denoted as extralattice oxygen (ELO), has special properties. It catalyzes the $O_2/^{18}O_2$ oxygen exchange reaction over Fe-ZSM-5 at room temperature (12).

From $N_2{}^{18}O$ studies over Fe-Mor it appeared that this oxygen was exchanged with lattice oxygen and with N_2O (Eq. [9]) (10). The latter can be interpreted as a nonproductive step compared to that of Eq. [7], and corroborates the possibility of this latter step:

$$N_2{}^{18}O + O^* \leftrightarrow N_2O + {}^{18}O^*. \quad [9]$$

For each ELO two Fe ions are involved (18, 19), but with N_2O about 1 oxygen is deposited per 4–5 Fe ions (12). On the other hand, more than eight times the maximum ELO capacity could be exchanged with lattice oxygen (10), indicating that this deposited oxygen readily loses its identity. The isolated nature of the ions in the zeolite framework resembles the dilute solid solution oxide systems, extensively studied two decades ago for the N_2O decomposition (20, 21). The mechanistic proposals made for these systems (20) may apply to zeolites, too (3). In essence, the oxygen moves from the transition metal (TM) ion to a matrix oxygen, becoming a peroxy-oxygen, and either reacts with another such oxygen to O_2, or with a newly incoming oxygen on the TM ion. For zeolites Hall *et al.* called the TM ion a "porthole." The identity of the oxygen may be lost by exchange with the framework oxygen. If the peroxy-oxygen is not mobile the reaction is limited to the direct vicinity of the TM ion, which is suggested by the value of four to five exchangeable lattice oxygens per Fe ion. A similar exchange of lattice oxygen with $N^{18}O$ was observed over Cu-ZSM-5 (10, 22). Recently, isotopic exchange reactions were reported between adsorbed $^{15}NO_2$ and NO over Co- and Cu-ZSM-5, which indicate a rapid exchange of the nitrogen (23).

Recently, we compared qualitatively the behavior of three zeolitic catalysts in the N_2O decomposition, viz. Co-, Cu-, and Fe-ZSM-5, and found striking differences (11) with respect to activity, inhibition, and pressure dependency. Here, we focus on the quantitative interpretation of the data to give a detailed microkinetic model for these catalysts.

2. EXPERIMENTAL

2.1. Catalysts

Cu-, Fe-, and Co-exchanged ZSM-5 zeolites have been used as catalysts for the N_2O decomposition. ZSM-5 zeolite ($SiO_2/Al_2O_3 = 37.2$) in the sodium form (ZEOCAT PZ-2/40 Na; Chemie Uetikon) was ion-exchanged, under vigorous stirring, using aqueous solutions (pH between 5.5 and 6) of Cu(II) acetate (4.0 m*M* at 293 K), Fe(II) sulfate (3.7 m*M* at 343 K), or Co(II) acetate (39.7 m*M* at 323 K). The zeolites were then filtered and washed thoroughly with deionized water at room temperature before drying at 383 K overnight. The metal content was determined by ICP-AES and AAS. The exchange levels were calculated on the basis of the amount Na^+ disappeared and the amount of transition metal TM introduced as Cu^{2+}, Fe^{3+}, or Co^{2+}. The data are given in Table 1.

2.2. Experimental Setup and Procedures

The experimental setup for N_2O decomposition consisted of a gas mixing section, a reactor and a gas analysis section. A quartz fixed bed reactor of 5 mm i.d. was used, containing 20–100 mg of catalyst (106–212 μm) diluted with 180 mg of SiC (106–212 μm), to assure plug flow, and operated at a total pressure of 2.5 bar.

The SiC diluent did not contribute to the N_2O decomposition at the reaction temperatures applied. Prior to each run, the catalyst was subjected to heating in He at 30 K/min to 923 K and maintaining this temperature for 1 h. Subsequently, the temperature was decreased to the desired value and the feed mixture was passed over the bed. Generally, 40 to 50 min after a change of conditions the conversion levels were constant and considered as the steady-state values. At least five analyses were averaged for a data point.

The product gases were continuously analyzed for NO and NO_2 using a chemiluminescence analyzer, and

TABLE 1

Catalysts Used

Sample	Metal loading (wt%)	Metal exchange level (%)
Cu-ZSM-5	4.0	130
Co-ZSM-5	1.6	73
Fe-ZSM-5	1.3	98

discontinuously for N_2O, N_2, CO, CO_2, and O_2 by GC equipped with a thermal conductivity detector and an electron capture detector, specifically for the N_2O analysis, using a Poraplot Q column and a molsieve 5A column for separation.

Conditions. The influence of temperature, partial N_2O and O_2 pressure, space time W/F_{N_2O}, and gases like CO and NO on the decomposition of N_2O over the catalysts were studied. The temperatures varied between 625 and 873 K. The inlet partial N_2O pressure ranged from 0.5 to 2 mbar, the O_2 pressure from 0 to 100 mbar, and the space time from 1.5×10^5 to 11.0×10^5 g · s/mol. The total gas flow rates were between 1 and 5 ml (STP)/s. NO or CO was added in molar ratios of 0–2 with N_2O (kept at 1 mbar). The low partial pressures were obtained by using gas mixtures of 5% in He and further dilution with helium by means of mass flow controllers.

Parameter estimation. Integral reactor behavior was used for the interpretation of the experimental data. To this purpose the reactor continuity Eq. [10] was integrated numerically using the Bulirsch–Stoer method (24) to calculate the exit conversion of nitrous oxide. In Eq. [10] r_{N_2O} represents the expression for the total N_2O conversion rate, as will be derived under Discussion:

$$\frac{dx_{N_2O}}{d\left(\frac{W}{F^0_{N_2O}}\right)} = r_{N_2O}. \qquad [10]$$

The apparent rate parameters were estimated by nonlinear least-squares methods (Simplex (25) and Levenberg-Marquardt (26, 27)), minimizing the sum of squares of the residual (= observed–calculated) N_2O conversion. The temperature dependency of the rate parameters was expressed in the Arrhenius form. The confidence limits of the parameter estimates were calculated from their covariance matrix at the 95% confidence level (28, 29). Transport limitations could be neglected (30).

3. RESULTS

An impression of the activity of the different catalysts is given in Fig. 1. The activity order Cu > Co > Fe corresponds with literature (6). The N_2O pressure dependency for Co-ZSM-5 is given in Fig. 2. Due to the integral reactor behavior the relation between conversion and partial pressure shows a curvature, but the reaction order equals 1 for Co and Fe below 733 K, while lower values are found for Cu and for Fe at higher temperatures. The fitting results of apparent activation energies for the different experiments, assuming a first order behavior, are given in Table 2. Included in this table are also the apparent reaction orders for a combined fit of the whole data set for an assumed *n*th order behavior. Full results are available through the authors on request.

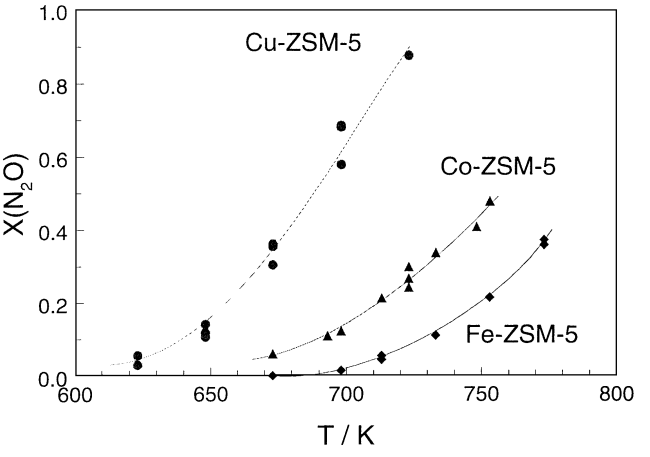

FIG. 1. Conversion as a function of temperature at 1 mbar N_2O and space time 1.44×10^5 g · s/mol for Co-, Cu-, and Fe-ZSM-5.

The presence of O_2 hardly affects the reaction over Fe- (at lower temperatures) and Co-ZSM-5, but it inhibits for the Cu system and for Fe at higher temperatures (Fig. 3). The apparent E_a for Cu increased by nearly 40 kJ/mol.

Addition of CO enhances the N_2O conversion, by about a factor of two for Co and tremendously for Fe (Fig. 4). In the latter case N_2O is being converted at temperatures where in absence of CO hardly any conversion is being observed. For Cu a maximum in the N_2O conversion appears as a function of the CO/N_2O ratio in the feed. This maximum shifts to higher values with increasing temperature (Fig. 5). The apparent activation energy for Co is hardly altered; for Fe it decreased nearly 100 kJ/mol, while for Cu it is increased by 50 kJ/mol.

The product distribution over Fe-ZSM-5 (Fig. 6a) clearly shows the 1:1 stoichiometry for the reaction between N_2O and CO (Eq. [11]). Over Cu-ZSM-5 at low CO

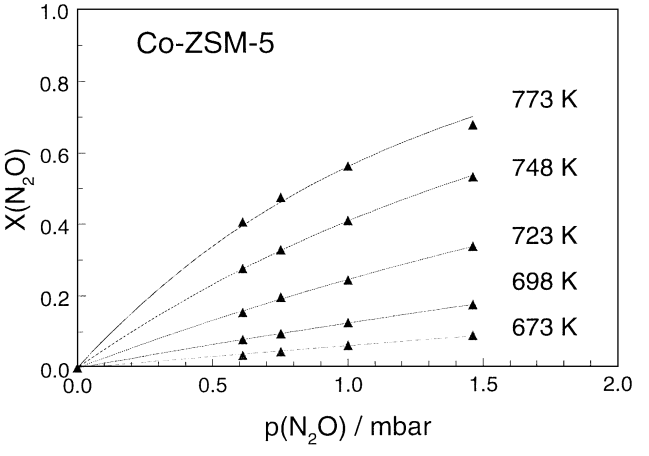

FIG. 2. N_2O conversion as a function of N_2O pressure for Co-ZSM-5 at various temperatures and a space time of 1.52×10^5 g · s/mol. Drawn lines are the model fits.

TABLE 2

Apparent Activation Energies (kJ/mol) and Reaction Orders[a]

	Only N_2O	O_2/N_2O = 30	CO/N_2O = 2	NO/N_2O = 1.5	All data	
					E_a	Order n
Co	104 ± 7	110	122	134	106 ± 15	1.00 ± 0.07
Cu	136 ± 38	175	179	138	138 ± 17	0.88 ± 0.11
Fe	168 ± 22	187	78	—	182 ± 31	0.79 ± 0.15

[a] 95% Confidence limits; 1st order assumed, except for the combined data set.

concentrations still some oxygen is observed (Fig. 6b), so both reactions of Eqs. [1] and [11] can occur simultaneously, depending on the conditions:

$$N_2O + CO \rightarrow N_2 + CO_2. \qquad [11]$$

Also addition of NO enhances the N_2O conversion over Fe-ZSM-5 tremendously and does not affect that for the other two catalysts (Fig. 7). It is, however, noted that NO is converted to NO_2 not only over Fe-ZSM-5, but also over Co-ZSM-5. The product composition for these two catalysts is given in Figs. 8a and 8b. Again it is noted that over Fe-ZSM-5 the conversion of N_2O occurs at temperatures where the decomposition does not noticeably take place without NO. NO is converted to NO_2 according to Eq. [12], while still O_2 formation takes place:

$$N_2O + NO \rightarrow N_2 + NO_2 \qquad [12]$$

4. KINETIC MODELING AND DISCUSSION

The Cu-, Co-, and Fe-ZSM-5 catalysts are all active systems for the decomposition of N_2O, but their behavior differs with respect to conditions and gas atmospheres. They all seem to obey a (nearly) first order dependency toward p_{N_2O},

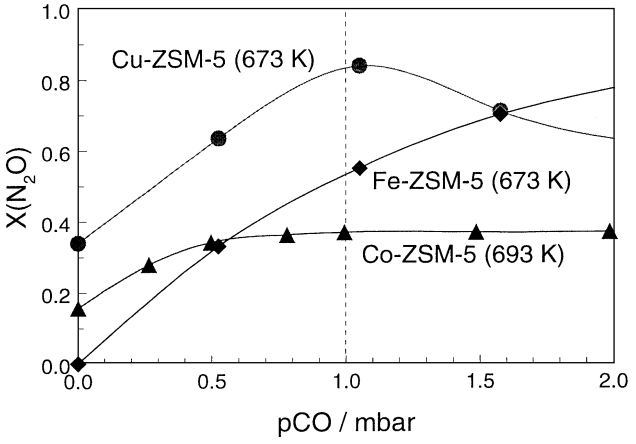

FIG. 4. The effect of CO on the N_2O conversion at 1 mbar N_2O and space time $W/F_{N_2O} = 1.52 \times 10^5$ g · s/mol. Drawn curves are model fits.

which can be rationalized by the two-step kinetic model given by Eqs. [6] and [7]. Their different behavior becomes especially apparent in their sensitivity to the presence of oxygen, of a reducing agent like CO, and even of NO. The enhancement by reducing agents can be expected only if they remove the oxygen deposited by the N_2O faster than occurs in the pure decomposition reaction. This competition must become apparent in the kinetic modeling discussed below. The results of this modeling are given in Table 3 (parameter estimates) and Figs. 9a–9c (predicted versus observed N_2O conversions for all experiments). Assuming that all TM ions in the zeolite samples are active centers, so their concentration represents N_T, then from the rate parameters in Table 3 turnover rates of the various reaction steps in the kinetic models can be estimated for the hypothetical case that all sites participate in that step. These values are given in Table 4 for 1 mbar reactant pressures, where applicable, at the temperatures indicated. The

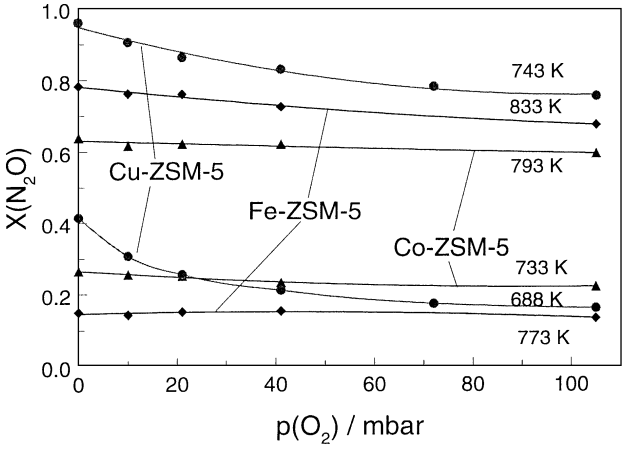

FIG. 3. The effect of oxygen on the N_2O conversion at 1 mbar N_2O and different temperatures. Space time $W/F_{N_2O} = 2.87 \times 10^5$ g · s/mol.

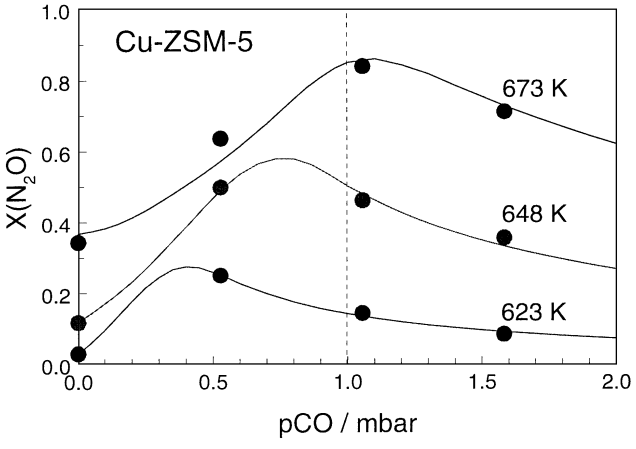

FIG. 5. Effect of CO on the N_2O conversion over Cu-ZSM-5 at 1 mbar N_2O and space time $W/F_{N_2O} = 1.52 \times 10^5$ g · s/mol. Drawn curves are model fits.

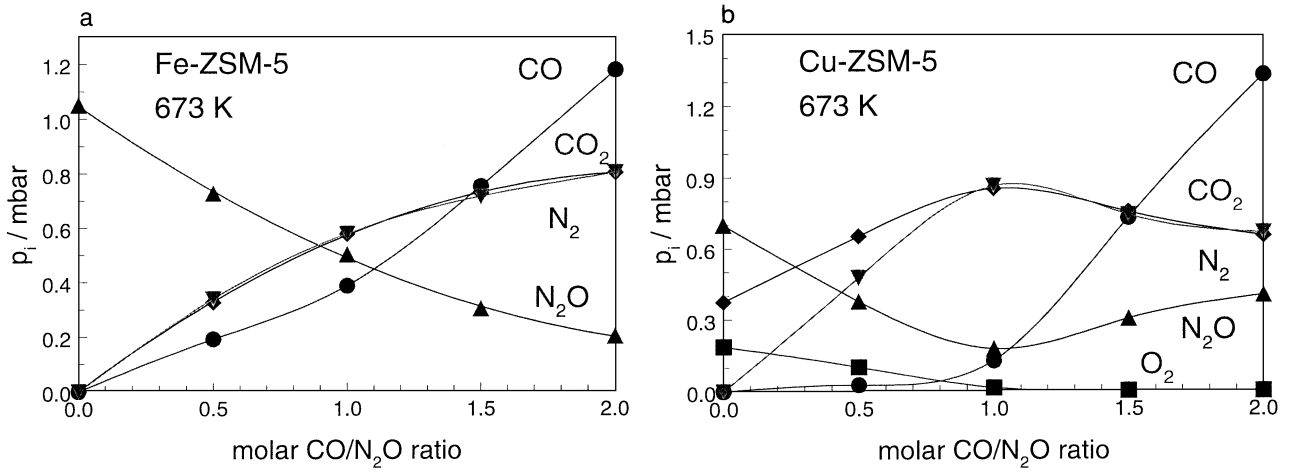

FIG. 6. Product composition for the CO/N_2O feed mixture at conditions of Figs. 4 over Fe-ZSM-5 (a) and Cu-ZSM-5 (b).

lowest values for a catalyst approach the turnover frequencies of the overall reaction for only N_2O. The other values represent in principle the maximum turnover frequency for that step if all sites would participate in that step. In reality the surface concentrations during steady-state operation will adjust in such a way that all steps turn over at rates in the catalytic cycle compatible with the overal reaction.

Co-ZSM-5

The experimental data of Co-ZSM-5 could be excellently described by the first order rate expression [8], with the parameter values given in Table 3. The observed conversion data are well predicted by this model (Fig. 9a). A first order rate expression could also be derived on the basis of the classical model if N_2O adsorption were the rate determining process. This would imply, however, that the surface oxygen occupancy is nearly zero and addition of a reducing agent like CO would not have any effect. Apparently it does have an influence, an argument in favor of the two-step model, formed by Eqs. [6] and [7].

The apparent rate constant contains the concentration of active sites, N_T (mol/g), and the two rate constants k_1 and k_2 of Eq. [8]. Assuming that all Co ions are active sites this results in turnover frequencies of 10^{-3}–10^{-2} s^{-1} (Table 4). A further determination of the individual values of the two rate constant was not possible on the basis of the data with N_2O alone. The experiment with CO addition, carried out at 693 K and two space times, gave additional information.

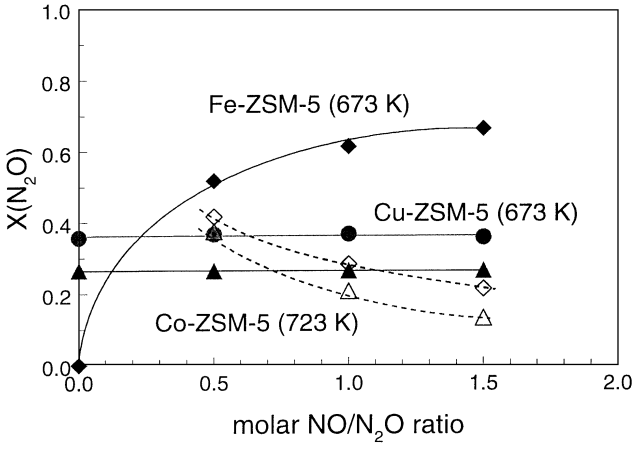

FIG. 7. Effect of NO on the N_2O conversion at 1 mbar N_2O and space time $W/F_{N_2O} = 1.52 \times 10^5$ g · s/mol. Included is the NO conversion (dashed lines and open symbols).

TABLE 3

Estimated Model Parameters and Their 95% Confidence Intervals[a]

Co-ZSM-5		
All data	$\ln(k_0 N_T) = 11.0 \pm 1.5$	$E_a = 104 \pm 7$
Data at 693 K	$2k_1 N_T = (0.17 \pm 0.03) \times 10^{-2}$	mol s^{-1} bar^{-1} g_{cat}^{-1}
(includ. CO)	$k_1/k_2 = 4.5 \pm 1.7$	—
	$k_4/k_2 > 40$	—
Cu-ZSM-5		
All CO data	$\ln(k_{02} N_T) = 17.7 \pm 0.2$	$E_{a2} = 136$[b]
	$\ln(k_{04} N_T) = -3.96 \pm 0.35$	$E_{a4} = 0$[b]
	$\ln(K_{05}\, k_{04}/k_{01}) = -19.0 \pm 3.0$	$\Delta H_5 + E_{a4} - E_{a1}$ $= -170 \pm 16$
All data at 673 K	$2k_2 N_T = (2.04 \pm 0.08) \times 10^{-3}$	mol s^{-1} bar^{-1} g_{cat}^{-1}
	$k_4 N_T = 0.0217 \pm 0.0038$	mol s^{-1} bar^{-1} g_{cat}^{-1}
	$K_5 k_4/k_1 = 1935 \pm 420$	bar^{-1}
	$k_2/k_3 = 413 \pm 39$	bar^{-1}
	$k_2/k_1 K_3 = 363 \pm 71$	bar^{-1}
Fe-ZSM-5		
N_2O data vs T	$\ln(k_{02} N_T) = 20.4 \pm 3.5$	$E_{a2} = 168 \pm 22$
CO data	$\ln(k_{04} N_T) = 6.55 \pm 1.10$	$E_{a4} = 64 \pm 6$
(623–713 K)	$\ln(k_{04}/k_{01}) = -1.16 \pm 0.08$	$E_{a4} - E_{a1} = -1.8 \pm 2.2$
NO data at 673 K	$k_7 N_T = 0.098$	mol s^{-1} bar^{-1} g_{cat}^{-1}
	$k_7/k_8 = 14$	—

[a] Activation energies E_{ai} in kJ/mol, $k_{0i} N_T$ in mol s^{-1} bar^{-1} g_{cat}^{-1}, K_5 in bar^{-1}, K_3 in bar.

[b] Fixed parameter value.

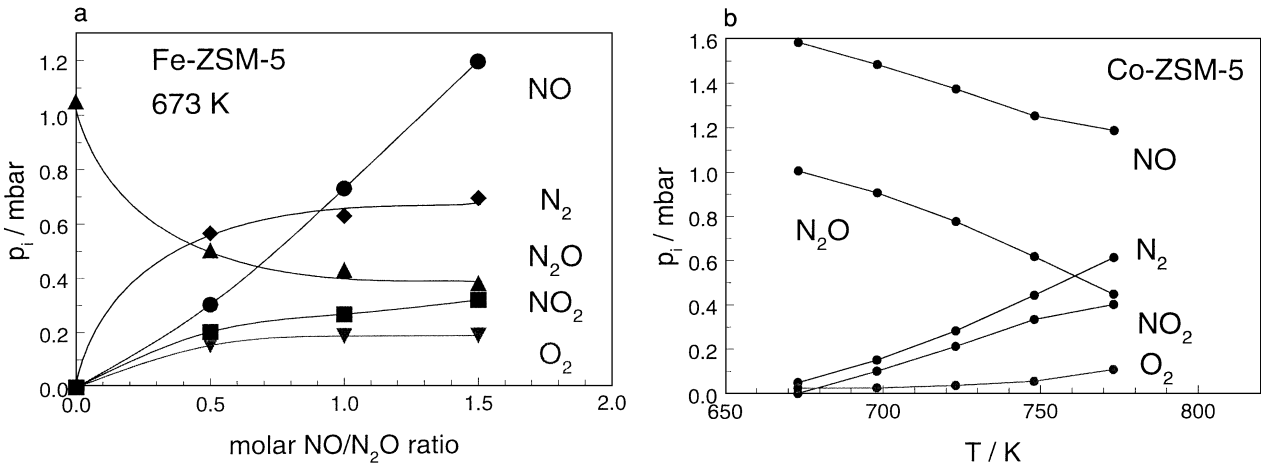

FIG. 8. Product composition for a NO/N_2O feed mixture at the conditions of Fig. 7 over Fe-ZSM-5 as a function of p_{NO} (a) and over Co-ZSM-5 as a function of temperature at 1 mbar NO (b).

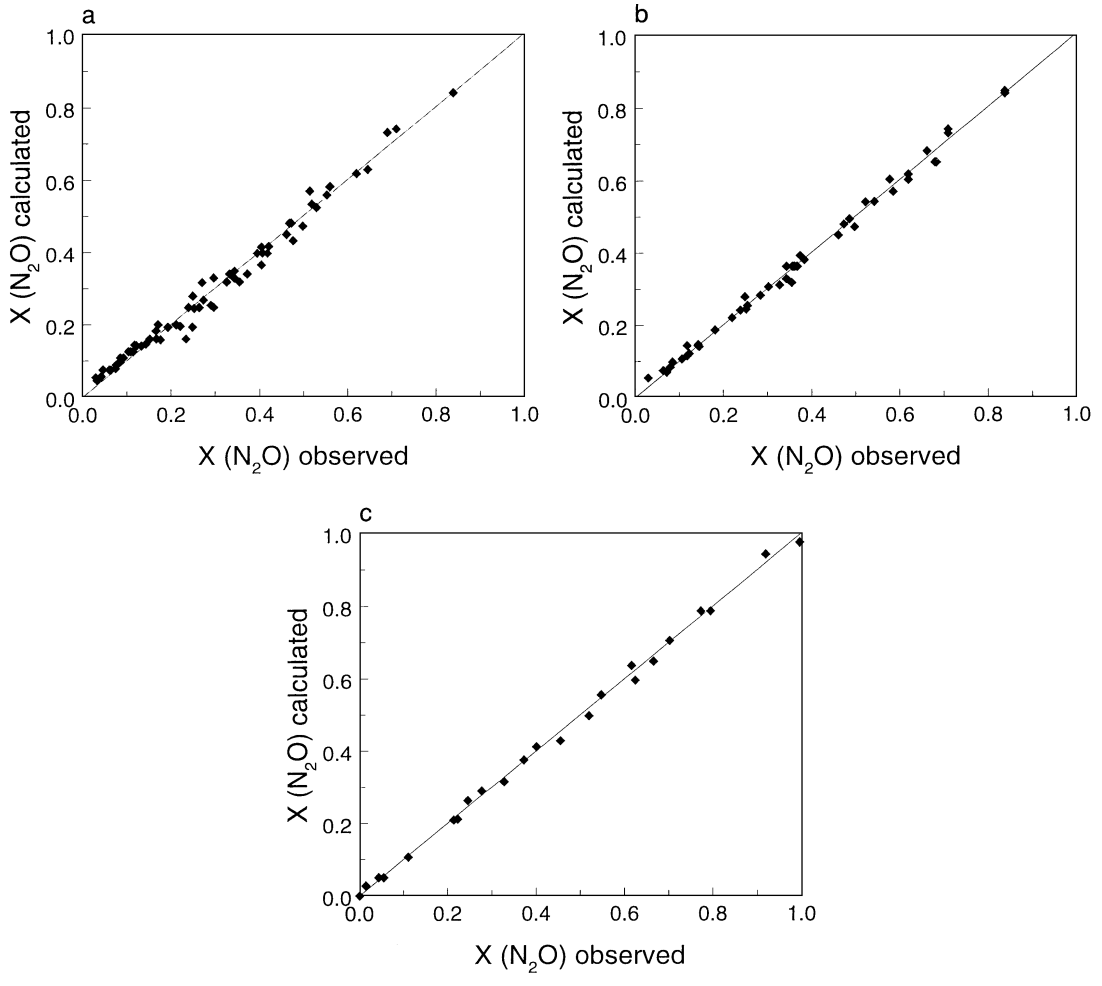

FIG. 9. Calculated model N_2O conversion as a function of the observed N_2O conversion for the data sets of Co-ZSM-5 (a), Fe-ZSM-5 (b), and Cu-ZSM-5 (c).

TABLE 4

Maximum Turnover Frequencies, TOF(max) (s^{-1}), Estimated for the Various Reaction Steps at 1 mbar Reactant Pressure (See Text)

Reaction step	From rate constant	TOF(max) (s^{-1}) Co-ZSM-5 (693 K)	Fe-ZSM-5 (673 K)	Cu-ZSM-5 (673 K)
Reaction* with N_2O, Eq. [6]	k_1N_T	6.1×10^{-3}	1.7×10^{-2}	
Reaction O* with N_2O, Eqs. [7], [21]	k_2N_T	1.4×10^{-3}	2.8×10^{-4}	1.6×10^{-3}
Desorption of O_2, Eq. [22]	k_3N_T			3.9×10^{-3}
O-removal by CO, Eq. [13]	k_4N_T	> 0.25	3.2×10^{-2}	3.4×10^{-2}
Reaction O* with NO, Eq. [17]	k_7N_T		0.4	

Apparently CO removes oxygen from the oxidized centers in competition with N_2O (Eq. [7]):

$$CO + O^* \xrightarrow{k_4} CO_2 + ^* . \qquad [13]$$

The resulting rate expression for the N_2O removal is now given by

$$r_{N_2O} = k_1 N_T p_{N_2O} \cdot \left\{ \frac{2 + \left((k_4/k_2) \cdot (p_{CO}/p_{N_2O})\right)}{1 + k_1/k_2 + \left((k_4/k_2) \cdot (p_{CO}/p_{N_2O})\right)} \right\}. \qquad [14]$$

For vanishing CO concentrations this reduces to Eq. [8], so the p_{CO}/p_{N_2O} terms in Eq. [14] account for the effect of CO in the N_2O destruction. Expression [14] contains three parameters that may be determined, k_1N_T, and the ratios k_1/k_2 and k_4/k_2. The parameter estimation yielded clear values for the first two, while for the latter ratio a lower limit was estimated. These results indicate that the rate constant of the oxidation step (Eq. [6]) is about 4.5 times larger than that of the removal by N_2O (Eq. [7]), whereas that for the removal by CO is about 10 times larger than for the oxidation step. For the reaction in only N_2O this means that about 80% of the active sites are in the oxidized state during decomposition, since the ratio k_1/k_2 represents the ratio between oxidized and empty sites, [O*]/[*]. The temperature dependency of the two rate constants did not differ that much to be able to determine their individual activation energies.

Fe-ZSM-5

The behavior of this catalyst is peculiar. At lower temperatures (<730 K) it exhibits first order behavior and no inhibition by oxygen, in agreement with earlier results (7, 8, 12). At higher temperatures the rate deviates from first order behavior and oxygen inhibition appears. The latter is in contrast with the results over oxidic catalysts, where inhibition decreases with temperature, for the obvious thermodynamic reason that adsorption is an exothermal process and less favored at higher temperatures. This is a support for the two-step model (Eqs. [6] and [7]) at lower temperatures. The increased sensitivity toward molecular oxygen is ascribed to the fact that at these temperature levels this catalyst starts to exhibit exchange reactions of molecular oxygen (12), indicating a dissociation of O_2. This implies an additional pathway, the reverse of Eq. [4], through which oxygen can be deposited on the active sites and which competes with the oxidation by N_2O. Hence, a gradually increasing inhibiting effect may be expected. The kinetic results above 730 K contained too little information to take this effect into account. Only the data below 730 K are used in the present kinetic analysis.

The data for N_2O alone can be considered as representative for the activation energy of the pure reaction (168 kJ/mol). The tremendous increase of the N_2O conversion in the presence of CO and NO indicates that the oxygen removal is the difficult step in the reaction and $k_1/k_2 \gg 1$, so in principle the rate of Eq. [7] is being measured in pure N_2O, as given by Eq. [15]. TOFs reported in literature range from 10^{-3} to 10^{-2} s^{-1} at 723 K (12), corresponding well with our data:

$$r_{N_2O} = 2k_2 N_T p_{N_2O}. \qquad [15]$$

For the results with CO the same kinetic approach holds as for Co-ZSM-5. Since now $k_2 \ll k_1, k_4$ the simplified expression that applies here is given by Eq. [16]. Estimated values for these parameters (623–713 K) are given in Table 3. Figure 9b shows that all N_2O conversions are well predicted by the modeling. The rate constants k_4 and k_1 are of the same magnitude and have about equal activation energies. The low value of the former (64 kJ/mol) explains the decrease in temperature dependency as indicated in Table 2 by the apparent activation energies. The results (Tables 3 and 4) indicate that the rate constant k_2 is two orders of magnitude smaller than k_4 and k_1.

$$r_{N_2O} = \frac{k_4 N_T p_{CO}}{1 + (k_4/k_1) \cdot (p_{CO}/p_{N_2O})}. \qquad [16]$$

Petunchi and Hall reported data on the CO–N_2O reaction over Fe-Mor and Fe-Y (16). They did not follow the kinetic approach presented here, but mentioned that the rate is dependent on the CO/N_2O ratio for Fe-Mor, with an activation energy of 76 kJ/mol, in agreement with our results (Table 2). The TOF for this catalyst at 673 K, 2.4 s^{-1}, is about 10 times higher than in our study. Fe-Y, being 500 times less active, exhibited a first order behavior in N_2O, which can be interpreted as $k_1 \ll k_4$ and the rate of the oxidation step of Eq. [6] is observed. These data indicate that for Fe the activity order for the zeolite matrices is Mor > ZSM-5 > Y.

This is not a general trend, because each TM ion has its own optimal zeolite matrix (3).

For the reaction with NO a similar approach can be followed as for CO, although it may be doubted whether the model should be modified or not. Both NO and NO_2 may adsorb at the active sites, as has been demonstrated by *in situ* DRIFTS experiments (11). Reduced Fe sites do not exist under these conditions as they are directly oxidized (11). The product NO_2 may be assumed to adsorb more strongly on the sites and it could be envisaged that desorption of NO_2 is enabled by the direct oxidation by N_2O, as has been observed for the desorption of CO_2 from oxidic catalysts effected by O_2 in the CO oxidation (31). The model becomes then the set of Eqs. [17] and [18]. Recently, an isotopic exchange study has been conducted between $^{15}NO_2$ and NO over Co-ZSM-5 and Cu-ZSM-5. Over Co-ZSM-5, which behaves similarly as Fe-ZSM-5 in the presence of NO, a rapid exchange between gaseous NO and adsorbed NO_2 was observed (23), which indicates an important role for adsorbed NO_2, like in the reactions of Eqs. [17] and [18]:

$$NO + O^* \xrightarrow{k_7} NO_2^* \qquad [17]$$

$$N_2O + NO_2^* \xrightarrow{k_8} N_2 + NO_2 + O^* \qquad [18]$$

$$r_{N_2O} = \frac{k_7 N_T p_{NO}}{1 + (k_7/k_8) \cdot (p_{NO}/p_{N_2O})}. \qquad [19]$$

The data do not allow an accurate estimation of the parameters in Eq. [19]; their values are highly correlated, but as an indication those for 673 K are included in Table 3, implying an even higher TOF(max) than with CO, 0.1–1 s^{-1} (Table 4). Thermodynamically the reaction of Eq. [12] allows complete conversion to NO_2 (3). This in contrast with the reaction between NO and O_2 which is equilibrium limited. The observed NO_2 levels are much above those according to this latter reaction, which evidences the reaction path of Eq. [12]. The observed formation of O_2 (Fig. 8) is expected on thermodynamic grounds. At these temperatures N_2O itself still does not yield O_2, and it is ascribed to the interaction of NO_2 with an oxidized site, schematically represented by Eq. [20]:

$$NO_2 + O^* \xrightarrow{k_9} NO + O_2 + {}^*. \qquad [20]$$

Cu-ZSM-5

The observed N_2O conversion data, apparent reaction order <1 and oxygen inhibition, can be well described by a rate expression of the form of Eq. [5], with either molecular (32, 33) or dissociative adsorption of oxygen. The latter is suggested by the NO dissociation properties especially for overexchanged Cu samples (e.g., Refs. 34, 35). Whether the presence of pairs or clusters of copper ions (32, 36) is essential remains to be answered, although it is a tempting explanation for the inhibition. Our Cu samples do have some overexchange (Table 1).

Assuming that for Cu the "classical" kinetic model should apply (Eqs. [2]–[4]), the rate parameter values indicate that the catalyst is not in a highly oxidized state at lower partial pressures and conversion levels. DRIFTS characterization data, however, show that the catalyst is in a highly oxidized state in the presence of N_2O (11). This suggests that desorption is a difficult step in the process, supported by the enhancement effect of CO.

An alternative kinetic model is proposed, formed by Eqs. [6], [21], and [22], in analogy to and as an extension of the two-step model for Co and Fe. The last step is reversible, but not assumed to be in quasi-equilibrium. The last step can be proposed on the basis of thermal desorption experiments of oxygen from different Cu-zeolites (22, 33, 37). In the NO decomposition it turned out that oxygen started to desorb only above 573 K (38), while in TPD experiments the peak maximum for O_2 desorption occurred around 673 K. This indicates that oxygen desorption is a difficult step in the process. The reversibility of this step is suggested by the observed O_2 inhibition here and for the NO decomposition (34, 37):

$$N_2O + {}^* \xrightarrow{k_1} N_2 + O^* \qquad [6]$$

$$N_2O + O^* \xrightarrow{k_2} N_2 + {}^*O_2 \qquad [21]$$

$${}^*O_2 \underset{k_{-3}}{\overset{k_3}{\rightleftarrows}} O_2 + {}^*. \qquad [22]$$

A suggestion for molecular O_2 adsorption follows from oxygen exchange experiments over Cu-ZSM-5. Cu exhibited most pronounced a single step double exchange reaction, i.e. $^{18}O_2$ was exchanged directly for O_2, without formation of singly labeled molecules, at the temperatures of interest here (22, 39). The model rate expression is given by Eq. [23] and includes the simplification that the concentration of empty sites is negligible compared to that of *O and $^*O_2$

$$r_{N_2O} = \frac{2k_2 N_T p_{N_2O}}{1 + (k_2/k_3) p_{N_2O} + (k_2/k_1 K_3) p_{O_2}}. \qquad [23]$$

Comparison of this rate expression with Eq. [5] indicates the similar form, but the interpretation of the parameters is different. The new model allows that the parameters in the denominator may increase with increasing temperature, in contrast to pure adsorption constants that thermodynamically only are allowed to decrease.

The experimental data did not allow a statistical distinction between a molecular or a dissociative oxygen adsorption model. The latter was found for NO decomposition (34, 37). Table 3 indicates values for the parameters in Eq. [23]

for a temperature of 673 K at which most of the experiments had been conducted. These include the partial pressure variation of N_2O and O_2 and the addition of CO. TOFs reported in literature for the O_2 desorption (37, 39) correspond to the values given in Table 4, 10^{-3}–10^{-2} s^{-1}.

For the enhancement by CO the model was extended with Eq. [13], the removal of oxygen, and Eq. [24], which represents the adsorption of CO at reduced sites and assumed to be in quasi-equilibrium. DRIFTS experiments have demonstrated the strong reversible adsorption of CO at Cu^{1+} sites at the applied conditions (11):

$$CO + {}^* \overset{K_5}{\longleftrightarrow} {}^*CO. \qquad [24]$$

The complete rate expression for this model is given by

$$r_{N_2O} = \frac{2k_2 N_T p_{N_2O} + k_4 N_T p_{CO}}{\left(1 + \frac{k_2}{k_3} p_{N_2O} + \frac{k_2}{k_1 K_3} p_{O_2}\right) + (1 + K_5 p_{CO})\left(\frac{k_2}{k_1} + \frac{k_4}{k_1} \frac{p_{CO}}{p_{N_2O}}\right)}. \qquad [25]$$

From the CO experiments it became clear, like in the case for Fe-ZSM-5, that $k_2 \ll k_1$ and that $1 \ll K_5 p_{CO}$, leaving a simplified expression for parameter estimation (Table 3):

$$r_{N_2O} = \frac{2k_2 N_T p_{N_2O} + k_4 N_T p_{CO}}{\left(1 + (k_2/k_3) p_{N_2O} + (k_2/k_1 K_3) p_{O_2}\right) + (k_4 K_5/k_1)\left(p_{CO}^2/p_{N_2O}\right)}. \qquad [26]$$

The squared partial CO pressure term in the denominator clearly accounts for the maximum in the N_2O conversion as a function of the CO partial pressure (Figs. 4 and 5). It indicates the need to first remove an adsorbed CO from a site before it can be oxidized by N_2O and reduced by a second CO in a consecutive reaction.

For the temperature dependent behavior of the N_2O–CO reaction only the last term in the denominator could be estimated, due to the limited data with N_2O and O_2 pressure variation at these temperatures. This model can describe all conversion data well as is apparent from Fig. 9c. Also the shift in the maximum with temperature for the N_2O–CO experiments is well described (Fig. 5). The values for the CO data set are included in Table 3, whereby the activation energy E_{a2} (no CO) was fixed at the value obtained for pure N_2O, and that of E_{a4} at zero, since its value statistically did not deviate from zero. This low value can be rationalized by envisaging that a CO molecule first adsorbs at an oxidized site before it reacts. The negative adsorption enthalpy can compensate a low activation energy for the subsequent step. Even an overcompensation is known in literature giving rise to negative apparent activation energies for the cracking of *n*-alkanes over ZSM-5 (17). The temperature dependency of the last term in the denominator of Eq. [26] corresponds to $\Delta H_5 + E_{a4} - E_{a1} = -168$ kJ/mol. Since the adsorption enthalpy ΔH_5 is negative, with a value of −40 to −60 kJ/mol estimated from infrared studies (11), and E_{a4} is negligible, the value E_{a1} for the first reaction step will amount to about 110–130 kJ/mol. It indicates that this is the easier step in the decomposition.

Over Cu-ZSM-5 steady-state NO_2 formation in the presence of NO is not observed. Speculation offers two explanations; either it is not formed or it decomposes back to NO. IR measurements show by the presence of a 2134 cm^{-1} band that NO_2 can be formed on Cu-ZSM-5 (34, 40), but from TPD experiments it appears that it decomposes rapidly in the range of 600–700 K (38). On the basis of isotopic exchange measurements nitrate structures are even proposed (23). So, in our case this could mean that NO_2 reacts with an oxidized site to NO and O_2 much more efficiently than over Fe-ZSM-5 or Co-ZSM-5, acting as an oxygen carrier, and hence competes with N_2O. Apparently, this does, however, result neither in an acceleration of the N_2O decomposition nor in a significantly changing temperature dependency (Table 2).

Evaluating the results presented above, a detailed kinetic picture of the decomposition of N_2O over the studied catalysts has been obtained. In the steady state the active sites in Fe- and Cu-ZSM-5 are nearly fully oxidized, while for Co ~80% of the sites are oxidized. From the literature it is well established that the former catalysts operate in an oxidation reduction cycle, Fe^{2+}/Fe^{3+} and Cu^{+}/Cu^{2+} (18, 19, 36). Co^{2+} in zeolites is hardly oxidized or reduced, but ESR studies on dilute solid solutions of Co in MgO indicate that Co^{3+}–O^{-} formation is possible, rapidly followed by a migration of the deposited oxygen to lattice oxygen and reduction back to Co^{2+} (41). A second deposited oxygen could then directly form molecular oxygen. The involvement of lattice oxygen as ELO carriers is receiving increasing suppport from studies with labeled NO and N_2O (10, 22). Our kinetic analysis, however, cannot yield insight in the detailed mechanism, but is in good agreement with these ideas.

All the reported apparent activation energy values are compatible with literature values for Fe-zeolites (5, 7, 12, 13) or dilute solid solutions of Co in MgO (42). The kinetic (and IR (11)) results with NO indicate that, like CO, it can remove the oxygen from the surface of the Co and Fe catalyst, too, thereby forming NO_2. The NO does adsorb on the Co catalyst, evidenced by IR, yielding a slight increase in apparent activation energy. So, although at 723 K no enhancement is observed, some is expected at higher temperatures. Kinetically, the blocking of sites by the observed NO adsorption by DRIFTS (11) on the Fe catalyst is negligible compared to the enhancement achieved by the oxygen removal effect.

The kinetic model proposed for Cu-ZSM-5 should be further evaluated by using lower exchange levels and

exploring the adsorption and desorption of molecular oxygen with these samples in more detail. For the sake of completeness it is emphasized at this point that the compatibility of the sets of elementary reaction steps with the observed kinetics does not prove but only substantiates the proposed kinetic models.

The observed NO_2 formation offers the potential use of these catalysts in nitric acid plants off-gas treatment, where about equal amounts of NO and N_2O are present. The produced NO_2 can be reused in the nitric acid process (3). Furthermore, it is obvious that application of these catalysts strongly depends on the composition of the gas that has to be treated and additional kinetic data on the inhibiting and deactivating effects of, e.g., H_2O and SO_2 are required (see, e.g., Refs. (43–46).

CONCLUSIONS

A detailed microkinetic model has been developed that quantitatively predicts N_2O decomposition over Co-, Fe-, and Cu-ZSM-5 catalysts as a function of partial pressures of N_2O and O_2, space time, and temperature and in the presence of CO and NO. Over Co- and Fe-ZSM-5 the reaction is first order in N_2O pressure and is not inhibited by O_2, while Cu-ZSM-5 suffers from O_2 inhibition. In the kinetic model basically N_2O oxidizes an active site and removes it in a second step, thereby forming O_2. This second step is the difficult one in all cases and addition of CO or NO enhances the conversion. CO is effective for all catalysts, but it inhibits the reaction over Cu-ZSM-5 at concentrations in excess of N_2O due to strong adsorption. NO also enhances the N_2O conversion rate over Fe-ZSM-5 and forms NO_2, like it does over Co-ZSM-5, but here without a net effect on the N_2O conversion rate.

ACKNOWLEDGMENT

These investigations have been supported by the European Union under Contract JOU2-CT92-0229 and JR-M by a Human Capital and Mobility grant. Dr. E. Ito is gratefully acknowledged for the catalyst samples.

REFERENCES

1. Crutzen, P. L., *J. Geophys. Res.* **76**, 7311 (1971).
2. Soete, G. G. d., *Rev. Inst. Franc. Petr.* **48**, 413 (1993).
3. Kapteijn, F., Rodriguez-Mirasol, J., and Moulijn, J. A., *Appl. Catal. B Env.* **9**, 25 (1996).
4. Centi, G., D'Angelo, S., and Perathoner, S., "Book of Abstracts," p. 177. Europacat II, Maastricht, The Netherlands, 1995.
5. Sobolev, V. I., Panov, G. I., Kharitonov, A. S., Romannikov, V. N., Volodin, A. M., and Ione, K. G., *J. Catal.* **139**, 435 (1993).
6. Li, Y., and Armor, J. N., *Appl. Catal. B Env.* **1**, L21 (1992).
7. Leglise, J., Petunchi, J. O., and Hall, W. K., *J. Catal.* **86**, 392 (1984).
8. Fu, C. M., Korchak, V. N., and Hall, W. K., *J. Catal.* **68**, 166 (1981).
9. Chang, Y.-F., McCarty, J. G., Wachsman, E. D., and Wong, V. L., *Appl. Catal. B Env.* **4**, 283 (1994).
10. Valyon, J., Millman, W. S., and Hall, W. K., *Catal. Lett.* **24**, 215 (1994).
11. Kapteijn, F., Mul, G., Marban, G., Rodriguez-Mirasol, J., and Moulijn, J. A., *in* "11th International Congress on Catalysis—40th Anniversary" (J. W. Hightower and W. N. Delgass, Eds.), Studies in Surface Science and Catalysis, Vol. 101, p. 641. Elsevier, Amsterdam, 1996.
12. Panov, G. I., Sobolev, V. I., and Kharitonov, A. S., *J. Mol. Catal.* **61**, 85 (1990).
13. Chang, Y.-F., McCarty, J. G., and Zhang, Y. L., *Catal. Lett.* **34**, 163 (1995).
14. Armor, J. N., and Farris, T. S., *Appl. Catal. B Env.* **4**, L11 (1994).
15. Kharas, K. C. C., Robota, H. J., and Datye, A., *in* "Environmental Catalysis" (J. N. Armor, Ed.), ACS Symposium Series, Vol. 552, p. 39. ACS, Washington, DC, 1994.
16. Petunchi, J. O., and Hall, W. K., *J. Catal.* **78**, 327 (1982).
17. Kapteijn, F., Moulijn, J. A., and Santen, R. A. v., *in* "Catalysis: An Integrated Approach to Homogeneous, Heterogeneous and Industrial Catalysis" (J. A. Moulijn, P. W. N. M. v. Leeuwen, and R. A. v. Santen, Eds.), Studies in Surface Science and Catalysis, Vol. 79, p. 69. Elsevier, Amsterdam, 1993.
18. Garten, R. L., Delgass, W. N., and Boudart, M., *J. Catal.* **18**, 90 (1970).
19. Dalla Betta, R. A., Garten, R. L., and Boudart, M., *J. Catal.* **41**, 40 (1976).
20. Stone, F. S., *J. Solid State Chem.* **12**, 271 (1975).
21. Cimino, A., *La Chimica e l'Industria* **56**, 27 (1974).
22. Valyon, J., and Hall, W. K., *J. Catal.* **143**, 520 (1993).
23. Beutel, T., Adelman, B. J., and Sachtler, W. M. H., *Appl. Catal. B Env.* **9**, L1 (1996).
24. Bulirsch, R., and Stoer, J., *Num. Math.* **8**, 1 (1966).
25. Nelder, J. A., and Mead, R., *Comput. J.* **7**, 308 (1965).
26. Levenberg, K., *Q. Appl. Math.* **2**, 164 (1944).
27. Marquardt, D., *SIAM J. Appl. Math.* **11**, 431 (1963).
28. Froment, G. F., and Hosten, L., *in* "Catalysis; Science and Technology" (J. R. Anderson, and M. Boudart, Eds.), Vol. 2, p. 97. Springer, Berlin, 1981.
29. Kapteijn, F., and Moulijn, J. A., *in* "Handbook of Heterogeneous Catalysis" (G. Ertl, H. Knözinger, and J. Weitkamp, Eds.), Vol. A. VCH, Weinheim, 1996.
30. Kapteijn, F., and Moulijn, J. A., *in* "Handbook of Heterogeneous Catalysis" (G. Ertl, H. Knözinger, and J. Weitkamp, Eds.), Vol. A. VCH, Weinheim, 1996.
31. Dekker, F. H. M., Dekker, M. C., Bliek, A., Kapteijn, F., and Moulijn, J. A., *Catal. Today* **20**, 409 (1994).
32. Jacobs, P. A., and Beyer, H. K., *J. Phys. Chem.* **83**, 1174 (1979).
33. Iwamoto, M., Maruyama, K., Yamazoe, N., and Seiyama, T., *J. Phys. Chem.* **81**, 662 (1977).
34. Valyon, J., and Hall, W. K., *J. Phys. Chem.* **97**, 1204 (1993).
35. Iwamoto, M., Yahiro, H., Mizuno, N., Zhang, W.-X., Mine, Y., Furukawa, H., and Kagawa, S., *J. Phys. Chem.* **96**, 9360 (1992).
36. Lei, G. D., Adelman, B. J., Sarkany, J., and Sachtler, W. M. H., *Appl. Catal. B Env.* **5**, 245 (1995).
37. Li, Y., and Hall, W. K., *J. Catal.* **129**, 202 (1991).
38. Li, Y., and Armor, J. N., *Appl. Catal.* **76**, L1 (1991).
39. Chang, Y.-F., Somorjai, G. A., and Heinemann, H., *J. Catal.* **154**, 24 (1995).
40. Hoost, T. E., Laframboise, K. A., and Otto, K., *Catal. Lett.* **33**, 105 (1995).
41. Indovina, V., Cordischi, D., Occhiuzzi, M., and Arieti, A., *J. Chem. Soc. Faraday Trans. 1* **75**, 2177 (1979).
42. Cimino, A., and Pepe, F., *J. Catal.* **25**, 362 (1972).
43. Dann, T. W., Schulz, K. H., Mann, M., and Collings, M., *Appl. Catal. B Env.* **6**, 1 (1995).
44. Li, Y., and Armor, J. N., *Appl. Catal. B Env.* **5**, L257 (1995).
45. Mabilon, G., and Durand, D., *Catal. Today* **17**, 285 (1993).
46. Li, Y., Battavio, P. J., and Armor, J. N., *J. Catal.* **142**, 561 (1993).